

# Clinical applications of superb microvascular imaging and virtual touch imaging quantification in pediatric mesenteric lymphadenitis diagnosis: A promising pathway to enhanced precision

Yi-Cheng Zhu<sup>a</sup>, Li Zhou<sup>a</sup>, Dao-Ming Zu<sup>b</sup>, Shu-Hao Deng<sup>a</sup>, Yuan Zhang<sup>a</sup>, Jun Shan<sup>a</sup>, Xiu-Rong Shi<sup>a</sup> and Quan Jiang<sup>a,\*</sup>

<sup>a</sup>*Department of Ultrasound, Pudong New Area People's Hospital Affiliated to Shanghai University of Medicine and Health Sciences, Shanghai, China*

<sup>b</sup>*Department of Pediatrics, Pudong New Area People's Hospital Affiliated to Shanghai University of Medicine and Health Sciences, Shanghai, China*

## Abstract.

**BACKGROUND:** Mesenteric lymphadenitis (ML) demonstrates a distinctive inclination for the pediatric and adolescent demographic and the diagnosis of ML in young children poses a substantial challenge.

**OBJECTIVE:** This prospective study aimed to assess the diagnostic efficacy of Superb Microvascular Imaging (SMI) and Virtual Touch Tissue Imaging quantification (VTIQ) in distinguishing pediatric mesenteric lymphadenitis.

**METHODS:** We examined 82 mesenteric lymph node (MLN) in pediatric patients with mesenteric lymphadenitis and 50 MLN in a healthy group. SMI was utilized to evaluate vascularity within the MLN, while MLN stiffness, quantified as shear wave velocity (SWV) in meters per second (m/s), was assessed using VTIQ. We compared the diagnostic performance of greyscale Ultrasound, US combined with SMI, US combined with VTIQ, and US combined with both SMI and VTIQ.

**RESULTS:** SMI revealed a significant distinction between mesenteric lymphadenitis and normal MLN ( $p < 0.001$ ). MLN affected by mesenteric lymphadenitis exhibited increased vascularity (marked vascularity: 13/82, 15.85%) compared to normal MLN (marked vascularity: 1/50, 2.00%). Statistically significant differences were observed in SWV values between mesenteric lymphadenitis and normal MLN (all  $p$ -values  $< 0.001$ ). The mean and minimum SWV values for MLN with mesenteric lymphadenitis were  $1.66 \pm 0.77$  m/s and  $1.51 \pm 0.53$  m/s, respectively. Control group SWV values were approximately three times higher than those in the mesenteric lymphadenitis group. The highest area under the curve values were achieved with the combination of all three modalities (0.837, 95% confidence interval: 0.763–0.896), followed by US + VTIQ (0.795, 0.716–0.860), US + SMI (0.753, 0.670–0.824) and US alone (0.642, 0.554–0.724).

**CONCLUSION:** SMI and VTIQ offer a promising noninvasive adjunct to grayscale ultrasound for identifying mesenteric lymphadenitis in pediatric patients.

Keywords: Mesenteric lymphadenitis, pediatrics, Elastography, Doppler ultrasound

## 1. Introduction

Mesenteric lymphadenitis (ML) demonstrates a distinctive inclination for the pediatric and adolescent demographic, manifesting a noticeably higher prevalence among males relative to females.

\*Corresponding author: Quan Jiang, No. 490, South Chuanhuan Road, Shanghai, China. Tel.: +86 21 20509048; E-mail: quan\_jmd@126.com.

Notably, this ailment bears a resemblance in terms of abdominal pain presentations to various pathological conditions, encompassing acute appendicitis, intestinal intussusception, and constipation [1]. Furthermore, akin to numerous instances of acute abdominal pain, mesenteric lymphadenitis frequently exhibits mild to moderate elevations in peripheral leukocyte count and C-reactive protein levels.

The diagnosis of ML in young children poses a substantial challenge due to the absence of distinct clinical manifestations and specific laboratory findings, often leading to mimicry of other diseases [2]. Additionally, it is frequently misconstrued as the primary cause of pseudoappendicitis [3]. Distinguishing ML from other conditions associated with abdominal pain remains a formidable task for pediatric practitioners. This diagnostic ambiguity or inadequate management has the potential to hinder timely identification and intervention, thereby significantly affecting early diagnosis and treatment in affected infants. Consequently, there is an imperative need to actively explore more precise and effective diagnostic approaches to enhance both diagnostic accuracy and therapeutic outcomes in pediatric cases of ML.

At present, there exists no universally accepted standard for defining mesenteric lymphadenopathy through grayscale ultrasound (US). In certain cases of appendicitis, substantial lymph node enlargement can also be detected via conventional US [4]. Evaluation data on asymptomatic pediatric mesenteric lymphadenopathy using conventional US is limited, and comprehensive studies on the size of mesenteric lymph nodes (MLNs) in normal children are lacking [5]. These factors, coupled with challenge in estimating MLNs in healthy children, contribute to a notably high rate of false positive when utilizing a short-axis diameter threshold of greater than or equal to 8 mm for the diagnosis of mesenteric lymphadenopathy in infants [2, 6].

The application of a sensitive Doppler technique, specifically known as Superb Microvascular Imaging (SMI), has exhibited superior capabilities in depicting extremely slow blood flow with heightened resolution and reduced artifacts in comparison to color Doppler and Power Doppler flow imaging [7–9]. ML is characterized by inflammation in the MLNs and is often seen in conjunction with inflammatory disorders or neoplasm. Additionally, prior publications indicated a potential link between ML and the development of new lymphoid vascularity [10, 11]. In terms of other imaging techniques, contrast-enhanced ultrasound (CEUS) is also often used in clinical practice to provide dynamic vascular imaging of very small vessels [12]. However, the use of ultrasound contrast agent in pediatrics is a major concern for their guardians and is still not approved by regulatory authorities [13]. Consequently, there are ongoing efforts to reduce radiation exposure in children. SMI aims to address these concerns.

The practice of palpation accompanied by an evaluation of tissue strain has long been a staple in abdominal examinations. Wherever palpation has demonstrated clinical value, elastography emerges as a pertinent diagnostic tool [14]. Consequently, the emergence of virtual tissue imaging quantification (VTIQ) has gained prominence in clinical practice and has been applied to various organs, including the thyroid [15], breast [16], liver [17], and lymph nodes [18]. A prior investigation has validated the efficacy of SMI in identifying ML in a pediatric population [19]. Therefore, our study aims to evaluate the diagnostic and prognostic value of integrating information about vascularity and stiffness in MLNs. The objective was to assess whether the correlation of findings from diverse imaging methods can augment diagnostic accuracy in this context.

## 2. Material and methods

This study was designed and collected at our Hospital after approval was obtained from our Ethics Committee (No.2021K43) and written consent was obtained from the parents of the participants who clinically diagnosed as ML in our hospital between June 2022 and June 2023. In total, 82 consecutive pediatric patients with ML were included. The children who agreed to participate in the study as

part of the ML cohort were required to meet specific inclusion criteria, which encompassed having a clinical diagnosis of ML and supplying complete imaging data. ML was defined as a clinical diagnosis on the discharge summary found in patients with right lower quadrant pain or tenderness, as well as based on sonographic findings of enlarged MLNs. Enlarged abdominal lymph nodes were specifically identified as those having a shortest diameter of 5 mm in the shortest diameter [1]. Patients with diagnosed appendicitis, cholecystitis, pancreatitis, and ileus were excluded from this study. Records of the laboratory tests, including white blood cell (WBC) count and the C-reactive protein (CRP) levels, were documented for analysis. Additionally, a control group of 50 healthy pediatric patients was also enrolled in this study as volunteers. The control cohort (N = 50) comprised 34 female children and 16 male children who volunteered to this study, all of whom had a median age of  $6.50 \pm 1.67$  years (range, 3–9 years) and were free of symptom during the US examination.

### 2.1. Image technique and evaluation

All MLNs in the ML cohort and control cohort underwent grayscale US, SMI, and VTIQ. US and SMI assessments were conducted using a Toshiba Aplio 500 (Toshiba Medical Systems Co., Tokyo, Japan) with a 14 MHz line array transducer. In both groups, all individual initially underwent an US examination, encompassing both transverse and longitudinal scans of the lower abdominal area. We meticulously documented the conventional ultrasound attributes, encompassing dimensions, shape, and echogenicity, for subsequent analysis. Dimensionality pertained to the maximal and minimal axes, whereas shape pertained to the proportion between the L and S axes, denoted as the L/S ratio. In the evaluation of vascular imaging parameters, the SMI technique was employed. The SMI velocity scope was adapted to less than 2.5 centimeters per second. Delicate transducer pressure was meticulously administered to ensure the vessels remained uncollapsed during the examination.

US assessments were conducted under the consistent guidance of an experienced radiologist, boasting over four years of expertise in abdominal US and two years of specialized experience in SMI. The interpretation of the vascularity index evaluated through SMI was entrusted to two additional radiologists, each possessing more than ten and twelve years of extensive background in abdominal imaging. In cases where interpretational discrepancies arose, a third distinguished radiologist, boasting an extensive background spanning over twenty years in abdominal US and three years in SMI, was summoned to facilitate a consensus-reaching process. This meticulous approach guaranteed the reliability and accuracy of the results.

The classification of vascular quantity was determined based on a calibrated scale. Vascular presence was categorized into four distinct levels: G0, representing a complete absence of blood flow; G1, indicative of minimal vascularity characterized by one or two pixels containing flow with a diameter of less than 0.1 cm; G2, denoting a moderate level of vascularity, signifying the presence of a defined amount of small vessels and/or a prominent main vessel; and finally, G3, which designated marked vascularity and was characterized by revealing more than 4 vessels within the region of interest (ROI). This classification scheme ensured precise and consistent evaluation of blood flow within the examined regions [20].

Afterwards, all enrolled patients received VTIQ examination, using a Siemens Oxana2 machine (Siemens Medical Solutions, Mountain View, CA, USA), equipped with a 9 MHz frequency 9L4 linear transducer. Consistency in the examination process was ensured by entrusting the same operator with the task of conducting all VTIQ examinations. To quantify shear-wave velocity (SWV) values, an ROI measuring  $2 \times 2$  mm was strategically positioned. Notably, SWV measurements were rigorously taken on seven occasions for each lymph node under scrutiny. In cases where the lymph node exhibited uniform stiffness distribution, the operator randomly positioned seven ROI boxes. In contrast, for lymph nodes displaying varying degrees of stiffness distribution, a meticulous approach was adopted. This

involved placing one SWV box in the softest region, another in the most stiff region, and the remaining five boxes positioned in a randomized manner [21]. Altogether, the study derived three distinct SWV values, namely, SWVMean ( $\pm$ standard deviation [SD]), SWVMax ( $\pm$ SD) and SWVmin ( $\pm$ SD).

## 2.2. Statistical analysis

To assess continuous variables, we applied either an independent *t*-test or the Mann-Whitney U test. Categorical variables were compared using the chi-squared test or Fisher's exact test. The comparison of vessel findings by SMI was conducted using the Wilcoxon rank-sum test. Receiver operating characteristic (ROC) curves were utilized to evaluate the diagnostic performance of clinical parameters (including temperature, WBC, and CRP), US alone, US+SMI, US+VTIQ, and US+SMI+VTIQ, with clinical confirmation by pediatrician serving as the gold standard. Statistical significance was defined as a *p*-value  $<0.05$ . SPSS 24.0 software (IBM, Armonk, NY, USA) was used to conduct statistical analysis

## 3. Results

### 3.1. Baseline characteristics

Out of a total of 85 patients in the mesenteric lymphadenitis cohort, 3 individuals were excluded from the analysis (Fig. 1). This exclusion stemmed from inadequate US imaging ( $n=2$ ) and technical complications during blood sampling ( $n=1$ ). Notably, there existed no significant distinctions in age or gender distribution between the two groups (both *p*-values  $>0.05$ ) (Table 1). In children afflicted with ML, common clinical manifestations encompassed a body temperature of  $37.8 \pm 0.76^\circ\text{C}$ , nausea (78.05%), vomiting (%), and anorexia (54.88%).

The WBC count ( $11.09 \pm 3.41 \times 10^9/\text{L}$  versus  $8.83 \pm 1.56 \times 10^9/\text{L}$ ), and CRP level ( $8.22 \pm 1.85$  mg/dL versus  $5.40 \pm 1.50$  mg/dL) in children with ML exhibited statistically significant elevations in comparison to their counterparts in the control cohort ( $p < 0.05$ ) (Table 1).

In children with ML, a total of 230 MLNs were identified, showing a median count of  $2.80 \pm 1.00$ . Conversely, in the cohort of healthy controls, 140 MLNs were detected, with a median count of  $2.80 \pm 1.11$ . It is noteworthy, however, that no significant disparity in the observed number of MLNs was ascertained between the two cohorts ( $p = 0.924$ ). It is also pertinent to mention that the echogenicity of all the identified MLNs was uniformly classified as either isoechoic or hypoechoic.

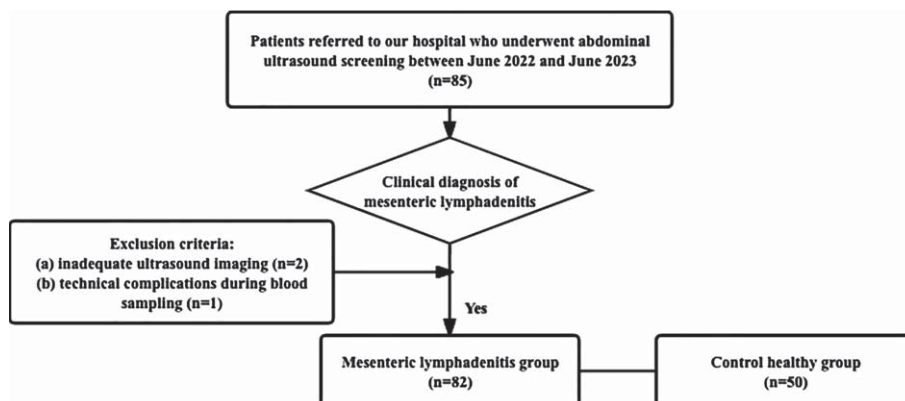


Fig. 1. Study cohort selection process.

Table 1  
Demographic and clinical parameters of children with mesenteric lymphadenitis and children in the control group

	ML group (n = 82)	Control group (n = 50)	p value
Age	6.08 ± 1.32	6.50 ± 1.67	0.116
Gender			0.499
Female	51	34	
Male	31	16	
Temperature (°C)	37.8 ± 0.76	36.7 ± 0.24	<0.001*
WBC (10 <sup>9</sup> /L)	11.09 ± 3.41	8.83 ± 1.56	<0.001*
CRP (mg/dL)	8.22 ± 1.85	5.40 ± 1.50	<0.001*
Duration of abdominal pain (days)	2.49 ± 1.24	N/A	N/A
Nausea	64 (78.05%)	N/A	N/A
Vomitting	40 (48.78%)	N/A	N/A
Anorexia	45 (54.88%)	N/A	N/A
Constipation	6 (7.32%)	N/A	N/A

WBC - white blood cell; CRP - C-reactive protein; ML - mesenteric lymphadenitis.

\*Indicates statistical significance.

Table 2  
Size and shape of enlarged mesenteric lymph nodes (MLNs)

	Longest diameter	Shortest diameter	L/S
ML group (n = 176)	1.30 ± 0.30	0.62 ± 0.11	2.18 ± 0.73
Control group (n = 101)	1.09 ± 0.22	0.56 ± 0.04	1.95 ± 0.42
p value	<0.001*	<0.001*	0.032*

ML - mesenteric lymphadenitis; L/S - longest diameter/shortest diameter. \*Indicates statistical significance.

Within the ML group, 73.48% (169/230) of the MLNs were found to be enlarged (Table 2). Conversely, in the control cohort, 66.43% (93/140) of MLNs exhibited enlargement. All the enlarged MLNs in children with ML were localized within the right lower quadrant. In the left lower quadrant, four healthy child displayed 9 out of 93 enlarged MLNs. The dimensions of MLNs in children with ML outstripped those in the control cohort. In children with ML, the longest diameter, the shortest diameter, and the ratio between the longest diameter and shortest diameter of the MLNs were markedly greater than those observed in the healthy cohort (all *p*-values <0.05).

### 3.2. Vascular observations

A significant difference in vascularity indices was evident between the two study cohorts. Within the ML group, SMI detected blood vessels in 89.02% (73/82) of the MLNs (Table 3). In stark contrast, only 46% (23/50) of MLNs in the control cohort displayed no discernible increase in vascularity. Furthermore, within the ML group, 52.44% (43/82) and 21.95% (18/82) of MLNs received G2 and G3 grades, respectively (Table 3). Conversely, in the control group, only 32% (16/82) and 2% (1/50) of MLNs received G2 and G3 grades.

Table 3  
Vascularity parameters

	G0	G1	G2	G3	z	p value
ML group	9	12	43	18	-5.192	<0.001*
Control group	23	10	16	1		

ML - mesenteric lymphadenitis. \*Indicates statistical significance.

Table 4  
Mesenteric lymph node stiffness findings

	SWV <sub>Min</sub>	SWV <sub>Mean</sub>	SWV <sub>Max</sub>
ML group	1.51 ± 0.53	1.66 ± 0.77	1.93 ± 0.44
Control group	4.38 ± 0.80	4.61 ± 1.20	4.88 ± 0.75
z	-9.607	-9.237	-9.603
p value	<0.001*	<0.001*	0.276

ML - mesenteric lymphadenitis; SWV - shear-wave velocity. \*Indicates statistical significance.

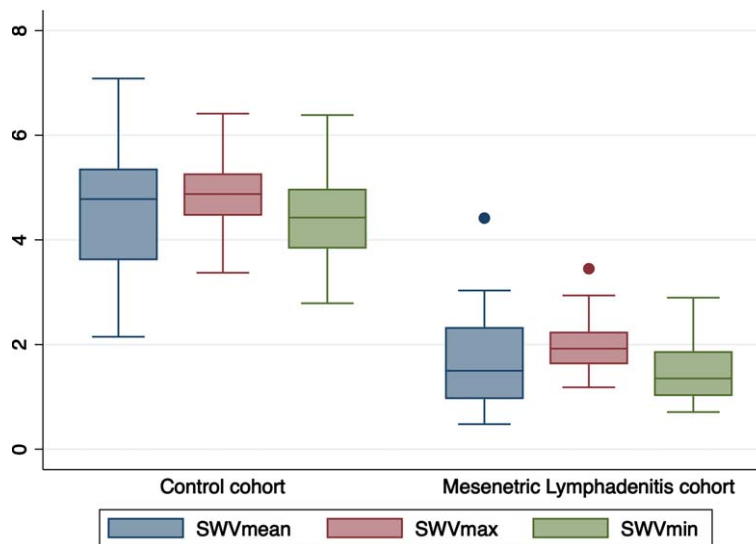


Fig. 2. Box plots showing shear-wave velocity measured in the mesenteric lymphadenitis group and the control group.

### 3.3. Stiffness observations

The mean SWV for the ML group stood at  $1.66 \pm 0.77$  m/s, while the control cohort exhibited a mean SWV of  $4.61 \pm 1.20$  (Table 4) (both  $p$ -values  $<0.001$ ). The SWV values in the control group were nearly threefold higher compared to those in the ML group (Fig. 2). Consequently, patients in the control group demonstrated stiffer MLNs in comparison to those afflicted with ML (Figs. 3 and 4).

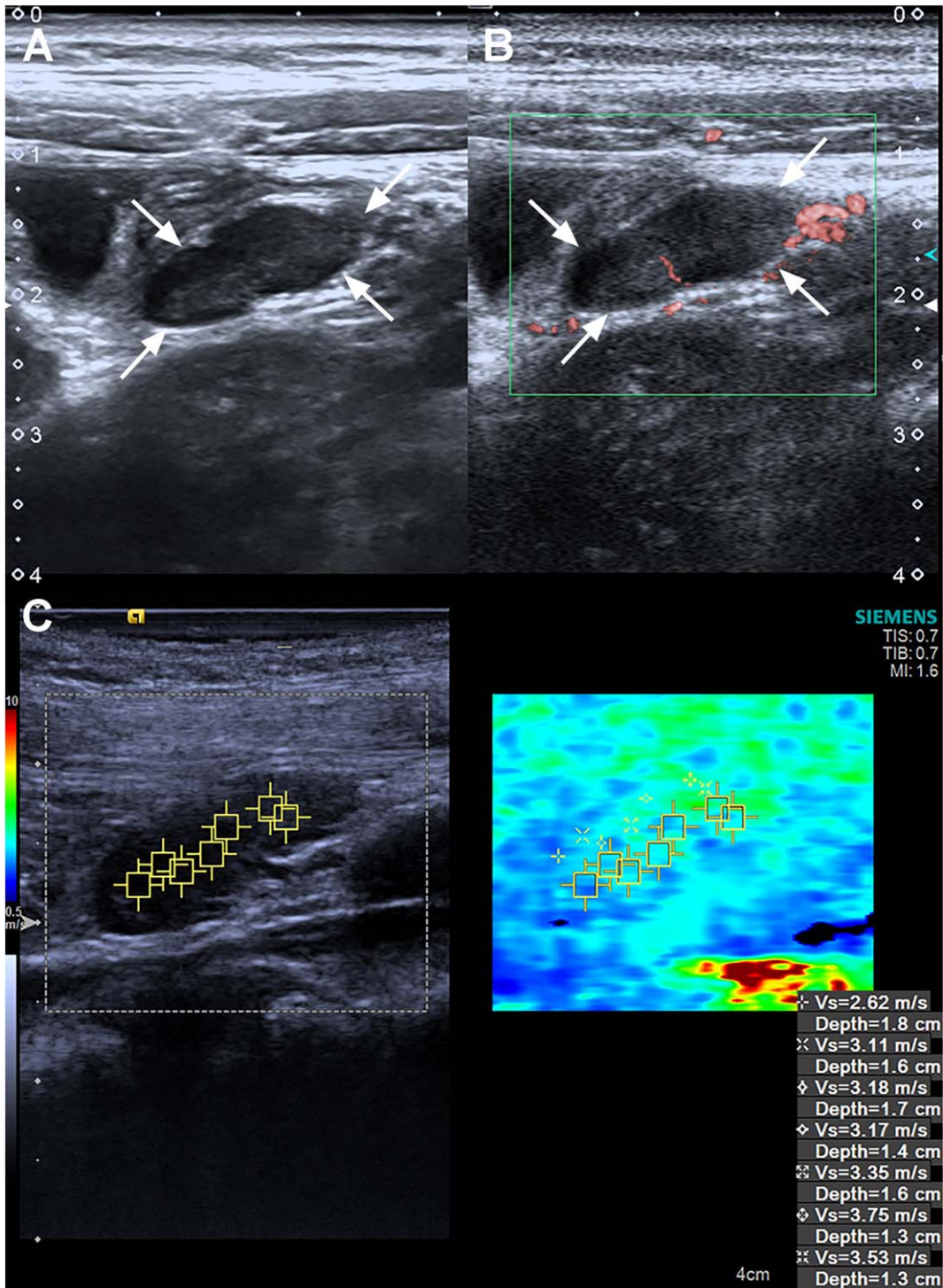


Fig. 3. Ultrasound, superb microvascular imaging and Virtual Touch imaging and quantification of a 5 years old pediatric female patient in the control group. (A) B-Mode ultrasound reveals it is a L/S <1 lymph node. (B) Superb microvascular imaging reveals it is an Adler G1 node. (C) Virtual Touch imaging quantification reveals the SWVMax, SWVMin, and SWVMean of the node is 3.75 m/s, 2.62 m/s, and 3.24 m/s. SWVMax = maximum shear-wave velocity, SWVMin = minimum shear-wave velocity, and SWVMean = average shear-wave velocity.

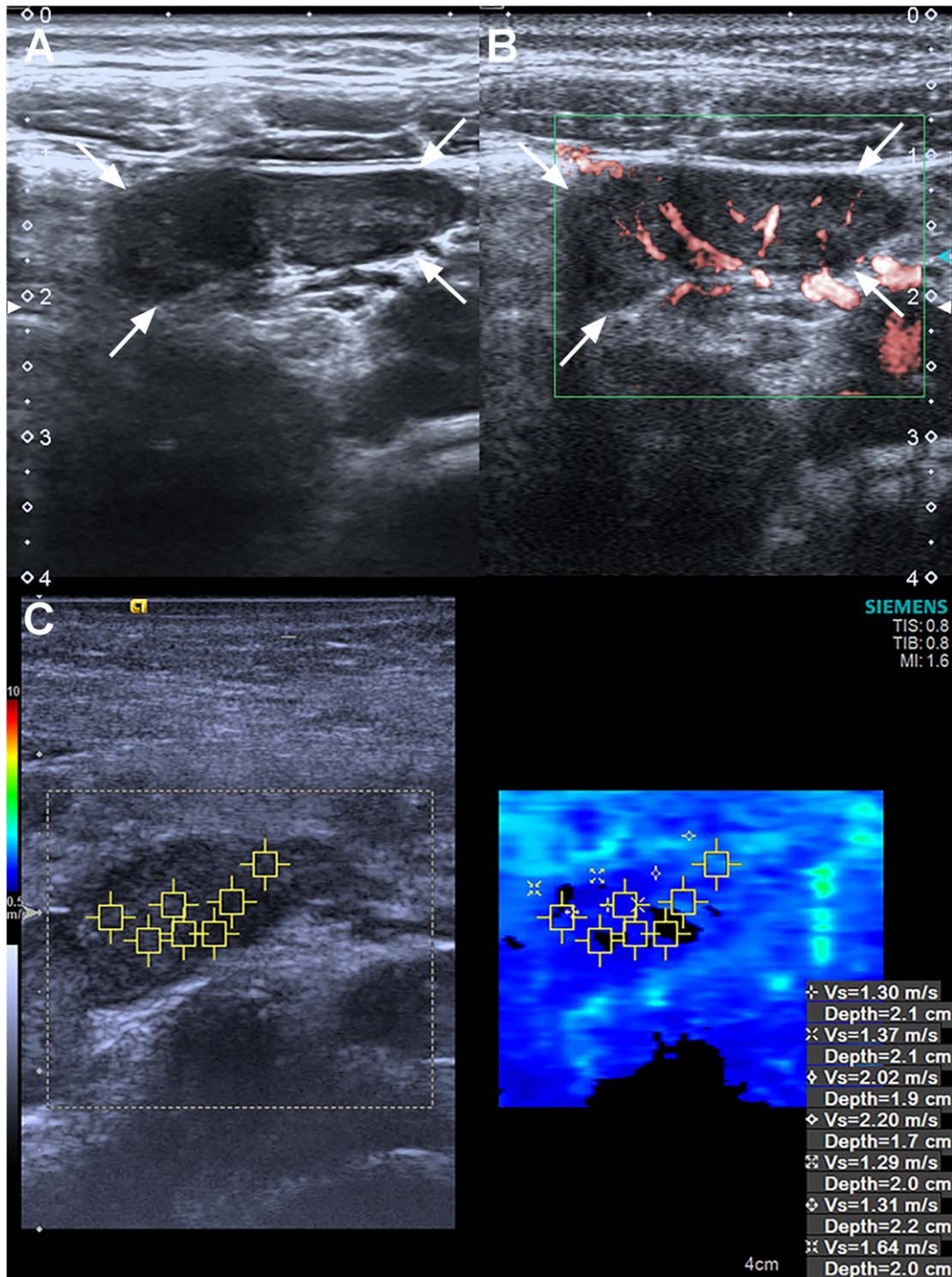


Fig. 4. Ultrasound, superb microvascular imaging and Virtual Touch imaging and quantification of a 7 years old pediatric male patient in the mesenteric lymphadenitis group. (A) B-Mode ultrasound reveals it is a  $L/S < 1$  lymph node. (B) Superb microvascular imaging reveals it is an Adler G3 node. (C) Virtual Touch imaging quantification reveals the SWVMax, SWVMin, and SWVMean of the node is 2.20 m/s, 1.29 m/s, and 1.59 m/s. SWVMax = maximum shear-wave velocity, SWVMin = minimum shear-wave velocity, and SWVMean = average shear-wave velocity.

Table 5  
Diagnostic performance of four modalities

	AUC	95% CI	Sensitivity	Specificity	Accuracy
Clinical parameters	0.426	0.325–0.528	29.27% (24/82)	50.00% (25/50)	39.40% (49/132)
US alone	0.642	0.554–0.724	80.49% (66/82)	48.00% (24/50)	68.18% (90/132)
US+SMI	0.753	0.670–0.824	86.59% (71/82)	64.00% (32/50)	78.03% (103/132)
US+VTIQ	0.795	0.716–0.860	89.02% (73/82)	70.00% (35/50)	81.82% (108/132)
US+SMI+VTIQ	0.837	0.763–0.896	91.46% (75/82)	76.00% (38/50)	85.60% (113/132)

AUC - area under the curve; CI - confidence interval; US - Grayscale Ultrasound; SMI - Superb microvascular imaging; VTIQ - Virtual Touch Imaging Quantification. \*Indicates statistical significance.

### 3.4. Diagnostic performance across different modalities

In the realm of ROC analysis, the most impressive AUC was achieved by the US+SMI+VTIQ combination, followed by US+VTIQ, US+SMI, US alone, and clinical parameters. The AUC values for these modalities were 0.837 (95%CI: 0.763–0.896), 0.795 (95%CI: 0.716–0.860), 0.753 (95%CI: 0.670–0.824), 0.642 (95%CI: 0.554–0.724), and 0.426 (95%CI: 0.325–0.528), respectively (Table 5). Notably, the US+SMI+VTIQ model had the best discriminative power to distinguish ML from healthy lymph nodes and yielded the highest sensitivity (91.46%) and specificity (76.00%) among all tested configurations.

## 4. Discussion

The diagnosis of ML in the pediatric population presents a significant challenge due to its high prevalence and unusual symptom presentation. However, relying solely on physical examinations or clinical parameters proves to be inadequate in identifying this condition. Moreover, given the increased risk of radiation-included malignancies associated with computed tomography scan in children, medical professionals consider ultrasound as the preferred imaging technique for diagnosing suspected cases of mesenteric lymphadenitis in pediatric patients. Our analysis revealed substantial differences in various clinical parameters related to vascular and stiffness findings between children with ML and their healthy counterparts. Specifically, in our study involving 132 children, ultrasound demonstrated a positive predictive value of 71.74% for ML. Moreover, when coupled with SMI and VTIQ, the positive predictive value increased to 86.21%. These findings underscore the importance of utilizing advanced ultrasound techniques in conjunction with traditional methods for improving diagnostic accuracy in pediatric cases of ML.

Inflammation, characterized by the dilation of small blood vessels and heightened microvascular permeability, plays a pivotal role in abdominal pain [22]. ML stands as a crucial indicator of the underlying inflammatory processes responsible for this pain. The advancement of Doppler technology has introduced a novel approach known as SMI. SMI incorporates an adaptive algorithm designed to precisely delineate both high- and low-velocity blood flow, offering superior resolution and minimizing motion artifacts in the process [23, 24]. In a prior investigation conducted by Bayramoglu et al. [25], the utility of SMI in assessing vascular blood flow in a pediatric and adolescent population ranging from 2 to 18 years was scrutinized. Their study included participants diagnosed with ML ( $n = 72$ ), lymphoma ( $n = 45$ ), and a cohort of healthy controls ( $n = 146$ ). Notably, the vascularity index derived through SMI displayed commendable diagnostic performance metrics, with sensitivity, specificity, and accuracy rates of 85%, 84%, and 85%, respectively, in the discrimination between ML and normal MLNs. The

diagnostic prowess of SMI, particularly in distinguishing ML from its normal lymphatic counterpart, is substantiated by these antecedent findings, with support from the vascularity index. Zu et al. [19] evaluated SMI in evaluating the microvasculature in 27 children with ML and 30 healthy children. They have adopted the same methodology as we did to grade vascularity findings. In their study, SMI showed 77.8% of MLNs of children with ML were graded as G2 (55.6%) and G3 (22.2%), whereas 76.7% of MLNs of healthy children revealed either no vascularity (56.7%) or minimal vascularity (20.0%). These previous findings align with the results of the current work, which employed a 4-level grading system to assess microvasculature using SMI. SMI detected blood flow signals in 89.02% of the ML group, with 21.95% of MLNs showing marked vascularity, visualizing more than four vessels within the ROI. In contrast, only 1 out of 50 MLNs in the healthy group exhibited marked vascularity.

Turning to the application of VTIQ, the advent of elastography and VTIQ has introduced the capability to qualitatively and quantitatively measure tissue elasticity and stiffness using shear waves. Elastography and VTIQ exploit shear waves to gauge tissue mechanical properties, particularly stiffness. In the case of soft tissue, the ease of shear wave deflection results in low velocities that can be measured. These SWVs can be assessed independently of the transducer's surface pressure. The feasibility of using elastography to classify lymph nodes has been published in the area of cervical lymph nodes [26] and superficial enlarged lymph nodes [27]. Our study demonstrates that SWV values increase from the mesenteric lymphadenitis group (SWVMean:  $1.66 \pm 0.77$  m/s) to normal lymph nodes (SWVMean:  $4.61 \pm 1.20$  m/s). This observation aligns with the notion that mesenteric lymphadenopathy may arise as a consequence of an underlying inflammatory process, potentially leading to softer tissue. Zhang et al. [28] also noted a comparable discovery. They studied 107 children exhibiting cervical lymph node enlargement and 60 healthy children without such enlargement. The elastic modulus values of children (average:  $10.8 \pm 2.0$  kPa) were observed to be lower than those of the healthy group (average:  $18.2 \pm 8.7$  kPa) ( $p < 0.01$ ). The researchers proposed that the samples included in their study were in an acute inflammatory edema phase, which aligned with similar cases observed in our work. Nevertheless, we acknowledge the existence of conflicting observations wherein the median elasticity and velocity metrics acquired via shear wave elastography exhibited a conspicuous elevation in instances of lymphoma as opposed to those with lymphadenitis and normal MLNs [25]. In consideration of these outcomes, we are committed to broadening the scope of our investigative endeavors by incorporating a substantial cohort of study samples spanning various centers. This endeavor aims to furnish a more exhaustive assessment of the discerned results.

In clinical practice, distinguishing between mesenteric adenitis and lymphoma presents a significant challenge due to overlapping characteristics in terms of size, shape, distribution, and Doppler imaging properties of lymph nodes [1, 22]. To address this diagnostic dilemma, a more accurate method is urgently required. This study represents the first attempt to investigate the diagnostic accuracy of combining SMI with VTIQ for distinguishing mesenteric lymphadenitis from a healthy group within a pediatric population. While Ultrasound alone exhibited relatively low specificity (48.00%), and accuracy (68.18%), the combination of either SMI or VTIQ improved these diagnostic parameters. Furthermore, when both SMI and VTIQ were employed in combination, the proposed approach demonstrated substantial promise in distinguishing between ML and normal MLNs. Notably, the combined modality reached the highest sensitivity (91.46%), specificity (76.00%), and accuracy (85.60%) when ultrasound served as the basis for assessment. This combination of imaging modalities presents a potential breakthrough in the accurate diagnosis of ML in the pediatric population, where such precision is imperative for clinical decision-making.

Our study has some limitations. First of all, the sample size of our study, although carefully selected, was relatively small, and the study was conducted at a single institution. Larger, multi-center studies are needed to validate our findings and establish broader applicability. Secondly, in this study, uniformity was maintained across all imaging examinations, with a single operator overseeing their execution.

However, it is noteworthy that ultrasonographic assessments and their subsequent interpretation exhibit a degree of sensitivity to the operator's proficiency. Consequently, forthcoming research endeavors should incorporate measures to mitigate potential interobserver and intraobserver disparities during the analysis of imaging results.

## 5. Conclusion

In summary, SMI is a non-invasive method without use of any contrast agents in identifying mesenteric lymphadenitis in a pediatric population. In this study, MLN with mesenteric lymphadenitis tended to be hypervascular. Additionally, VTIQ proved highly proficient in quantitatively measuring SWV. The lower the SWV, the more likely was mesenteric lymphadenitis. Therefore, the combined modality of SMI and VTIQ added to US proposed by our study suggests potential advantages in enhancing diagnostic accuracy for the detection of mesenteric lymphadenitis in a pediatric population.

## Acknowledgments

This study was supported by grants from the General Project Grant from the Pudong Health Commission of Shanghai (Grant No. PW2022A-05) and the National Natural Science Foundation of China (grant No. 82302231).

## References

- [1] Simanovsky N, Hiller N. Importance of sonographic detection of enlarged abdominal lymph nodes in children. *J Ultrasound Med.* 2007;26:581-4.
- [2] Toorenvliet B, Vellekoop A, Bakker R, Wiersma F, Mertens B, Merkus J, Breslau P, Hamming J. Clinical differentiation between acute appendicitis and acute mesenteric lymphadenitis in children. *Eur J Pediatr Surg.* 2011;21:120-3.
- [3] Ozdamar MY, Karavas E. Acute mesenteric lymphadenitis in children: Findings related to differential diagnosis and hospitalization. *Arch Med Sci.* 2020;16:313-20.
- [4] He L, Sun Y, Huang G. Identifying threshold sizes for enlarged abdominal lymph nodes in different age ranges from about 200,000 individual's data. *Sci Rep.* 2021;11:1762.
- [5] Cai B, Yi H, Zhang W. Reference intervals of mesenteric lymph node size according to lymphocyte counts in asymptomatic children. *PLoS One.* 2020;15:e0228734.
- [6] Karmazyn B, Werner EA, Rejaie B, Applegate KE. Mesenteric lymph nodes in children: What is normal? *Pediatr Radiol.* 2005;35:774-7.
- [7] Artul S, Nseir W, Armaly Z, Soudack M. Superb microvascular imaging: Added value and novel applications. *J Clin Imaging Sci.* 2017;7:45.
- [8] Ohno Y, Fujimoto T, Shibata Y. A new era in diagnostic ultrasound, superb microvascular imaging: Preliminary results in pediatric hepato-gastrointestinal disorders. *Eur J Pediatr Surg.* 2017;27:20-5.
- [9] Zhang C, Zheng C, Zhang Z, Yan X, Xu J, Gu C, Nie F. Quantitative analysis of contrast-enhanced ultrasound and superb microvascular imaging for the evaluation of disease activity in inflammatory bowel disease. *Clin Hemorheol Microcirc.* 2024. doi: 10.3233/CH-242114.
- [10] Costa C, Incio J, Soares R. Angiogenesis and chronic inflammation: Cause or consequence? *Angiogenesis.* 2007;10:149-66.
- [11] Liu N, Chen Y, Wang Y, Huang W, Zhan L, Du Z, Zhong Z, Wu Z, Shen Y, Deng X, Ni S, Tang L. A combination of ultrasound and contrast-enhanced ultrasound improves diagnostic accuracy for the differentiation of cervical tuberculous lymphadenitis from primary lymphoma. *Clin Hemorheol Microcirc.* 2023;85(3):261-75.
- [12] Chen X, Ma J, Fu Y, Mei F, Tang R, Xue H, Lin Y, Wang S, Cui L. Differential diagnosis of cervical lymphadenopathy: Integration of postvascular phase of contrast-enhanced ultrasound and predictive nomogram model. *Eur J Surg Oncol.* 2024;50:107981. doi: 10.1016/j.ejso.2024.107981.

- [13] Pschierer K, Grothues D, Rennert J, Platz Batista da Silva N, Schreyer AG, Melter M, Stroszczynski C, Jung EM. Evaluation of the diagnostic accuracy of CEUS in children with benign and malignant liver lesions and portal vein anomalies. *Clin Hemorheol Microcirc.* 2015;61:333-45. doi: 10.3233/CH-152003.
- [14] Gennisson J-L, Deffieux T, Fink M, Tanter M. Ultrasound elastography: Principles and techniques. *Diagn Interv Imaging.* 2013;94:487-95.
- [15] Zhang Y, Huang QY, Wu CJ, Chen Q, Xia CJ, Liu BJ, et al. Predicting malignancy in thyroid nodules based on conventional ultrasound and elastography: The value of predictive models in a multi-center study. *Endocrine.* 2023;80:111-23.
- [16] Wang A, Zhong J, Wang S, Wang H, Tao L, Wei H, et al. Different precompression does not reduce the diagnostic value of virtual touch tissue imaging and quantification (VTIQ) in breast lesions, especially for the ratio of the shear wave velocity between lesions and surrounding tissues. *Eur J Radiol.* 2022;151:110284.
- [17] Jung EM, Kaiser U, Herr W, Stroszczynski C, Jung F. Novel high-resolution contrast agent ultrasound techniques HiFR CEUS and SR CEUS in combination with shear wave elastography, fat assessment and viscosity of liver parenchymal changes and tumors. *Clin Hemorheol Microcirc.* 2024;86(3):263-73.
- [18] Choi YJ, Lee JH, Baek JH. Ultrasound elastography for evaluation of cervical lymph nodes. *Ultrasonography.* 2015;34:157-64.
- [19] Zu D-M, Feng L-L, Zhang L, Ma S-L, Zhu Y-C. Evaluation of mesenteric lymph nodes in a pediatric population with mesenteric lymphadenitis using superb microvascular imaging. *Med Sci Monit.* 2019;25:5336-42.
- [20] Adler DD, Carson PL, Rubin JM, Quin-Reid D. Doppler ultrasound color flow imaging in the study of breast cancer: Preliminary findings. *Ultrasound Med Biol.* 1990;16:553-9.
- [21] Sun JW, Wang XL, Zhao Q, Zhou H, Tao L, Jiang ZP, et al. Virtual touch tissue imaging and quantification (VTIQ) in the evaluation of breast lesions: The associated factors leading to misdiagnosis. *Eur J Radiol.* 2019;110:97-104.
- [22] Lucey BC, Stuhlfaut JW, Soto JA. Mesenteric lymph nodes seen at imaging: Causes and significance. *Radiographics.* 2005;25:351-65.
- [23] Machado P, Segal S, Lyshchik A, Forsberg F. A novel microvascular flow technique: Initial results in thyroids. *Ultrasound Q.* 2016;32:67-74.
- [24] Gabriel M, Tomczak J, Snoch-Ziolkiewicz M, Dzieciuchowicz L, Strauss E, Oszkinis G. Comparison of superb micro-vascular ultrasound imaging (SMI) and contrast-enhanced ultrasound (CEUS) for detection of endoleaks after endovascular aneurysm repair (EVAR). *Am J Case Rep.* 2016;17:43-6.
- [25] Bayramoglu Z, Caliskan E, Karakas Z, Karaman S, Tugcu D, Somer A, et al. Diagnostic performances of superb microvascular imaging, shear wave elastography and shape index in pediatric lymph nodes categorization: A comparative study. *Br J Radiol.* 2018;91:20180129.
- [26] Basiari L, Michali M, Litsou E, Psychogios G. Differential diagnosis of cervical lymph nodes with ultrasound and virtual touch imaging quantification: A report of three cases. *Maedica (Bucur).* 2023;18:148-52.
- [27] Ben Z, Gao S, Wu W, Chen S, Fu S, Zhang J, Chen Y. Clinical value of the VTIQ technology in the differential diagnosis of superficially enlarged lymph nodes. *Acta Radiol.* 2018;59:836-44.
- [28] Zhang X, Wang H, Ren H. The value of real-time shear wave elastography combined with conventional ultrasonography in the diagnosis of cervical lymphadenitis in children. *Acta Medicinæ Universitatis Scientiæ et Technologiæ Huazhaong.* 2022;51(4):545-9. [in Chinese]